

## Electronic Supplementary Information

### **Steric and electronic effects on arylthiolate coordination in the pseudotetrahedral complexes [(Tp<sup>Ph,Me</sup>)Ni-SAr] (Tp<sup>Ph,Me</sup> = hydrotris{3-phenyl-5-methyl-1-pyrazolyl}borate)**

Tapash Deb,<sup>a</sup> Caitlin M. Anderson,<sup>a</sup> Swarup Chattopadhyay,<sup>a</sup> Huaibo Ma,<sup>a</sup> Victor G. Young, Jr.<sup>b</sup>  
and Michael P. Jensen<sup>a,\*</sup>

<sup>a</sup>*Department of Chemistry and Biochemistry, Ohio University, Athens, Ohio 45701, USA and*

<sup>b</sup>*X-ray Crystallographic Laboratory, Department of Chemistry, University of Minnesota, Minneapolis, Minnesota 55455, USA.*

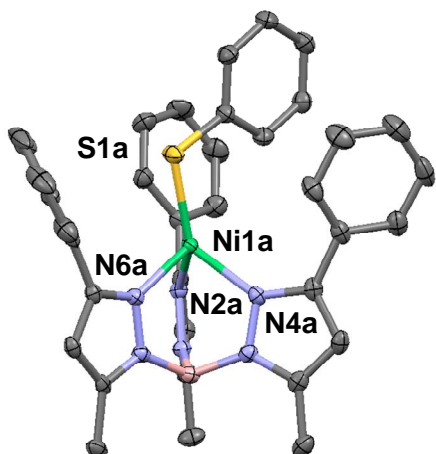


**Figure S1.** Thermal ellipsoid plot (50% probability) of  $[(\text{Tp}^{\text{Ph,Me}})\text{Ni-SPh}]$ . Hydrogen atoms are omitted for clarity. Relevant bond lengths for  $[(\text{Tp}^{\text{Ph,Me}})\text{Ni-SPh}]$  (Å): Ni1a–N2a, 2.005(2); Ni1a–N4a, 2.019(2); Ni1a–N6a, 2.013(2); Ni1a–S1a, 2.2224(7). Relevant bond angles for  $[(\text{Tp}^{\text{Ph,Me}})\text{Ni-SPh}]$  (°): N2a–Ni1a–N4a, 90.61(8); N2a–Ni1a–N6a, 91.66(8); N4a–Ni1a–N6a, 92.86(8); N2a–Ni1a–S1a, 129.21(6); N4a–Ni1a–S1a, 131.42(6); N6a–Ni1a–S1a, 109.85(6); Ni1a–S1a–C31a, 106.63(8).

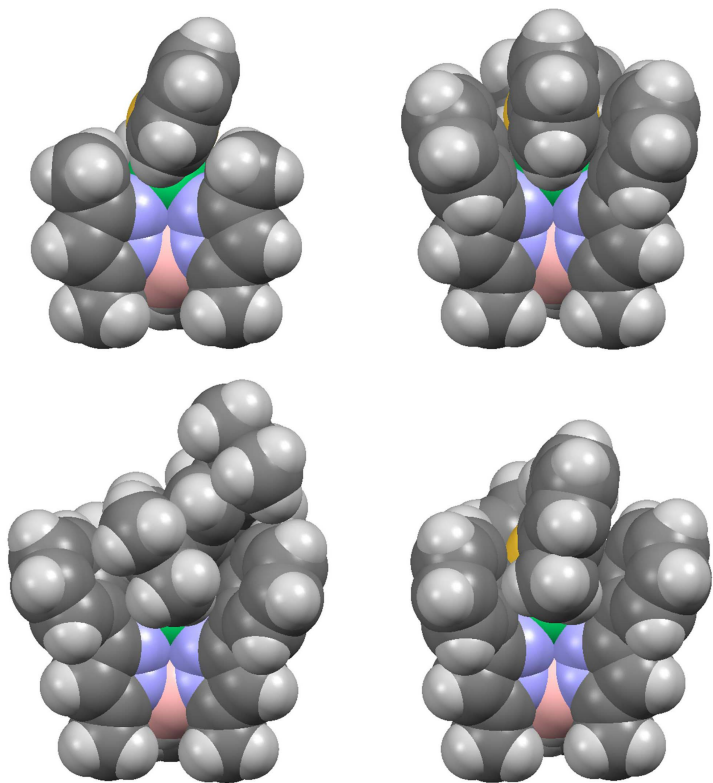


**Figure S2.** Space-filling diagrams (clockwise from top left) of  $[(\text{Tp}^{\text{Me,Me}})\text{Ni-SPh}]$ ,  $[(\text{Tp}^{\text{Ph,Me}})\text{Ni-SPh}]$ ,  $[(\text{Tp}^{\text{Ph,Me}})\text{Ni-S-2,6-Me}_2\text{C}_6\text{H}_3]$  and  $[(\text{Tp}^{\text{Ph,Me}})\text{Ni-S-2,4,6-}i\text{Pr}_3\text{C}_6\text{H}_2]$ .

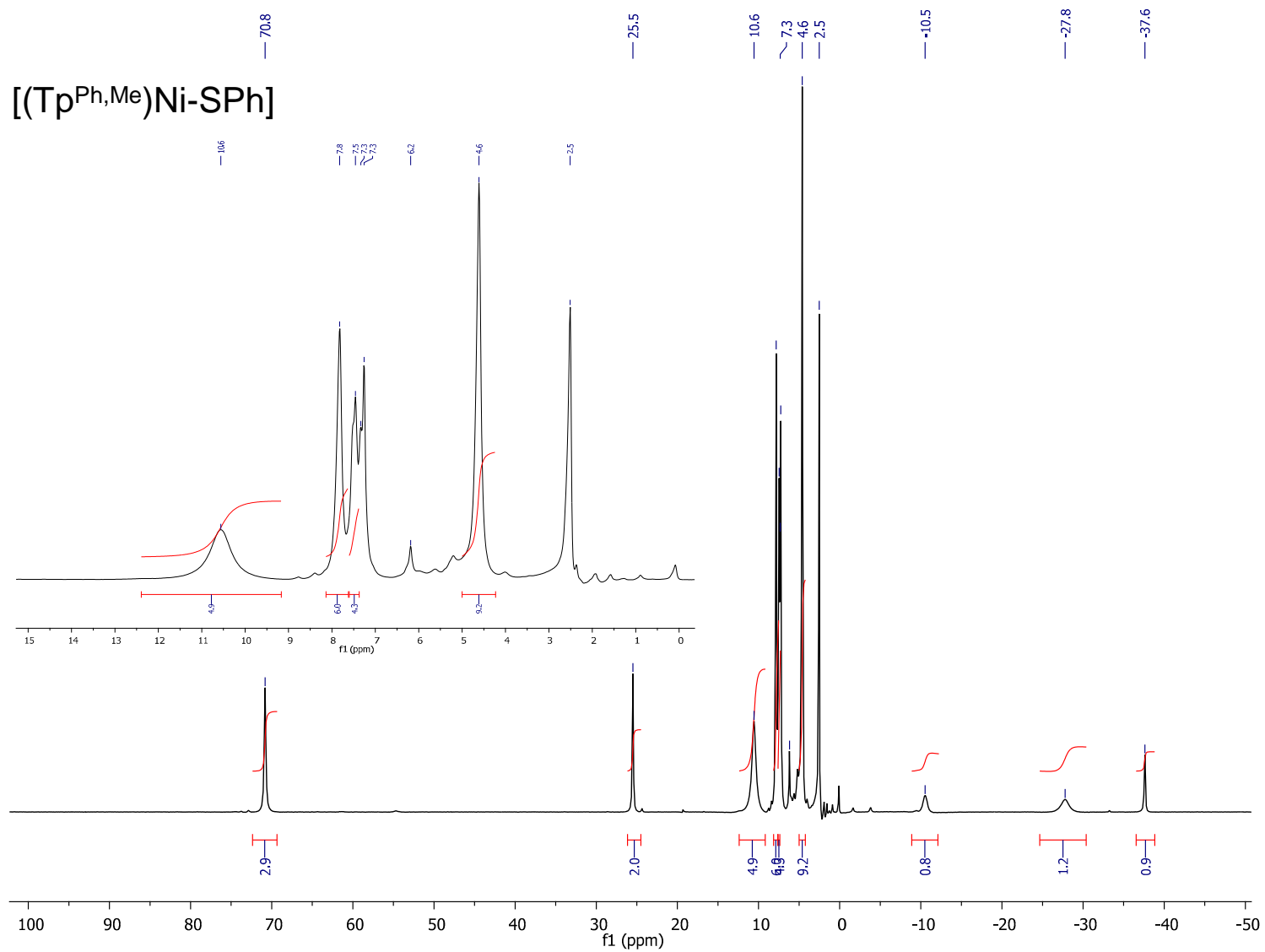


**Figure S3.** <sup>1</sup>H NMR spectrum (500 MHz, 295 K) of [(Tp<sup>Ph,Me</sup>)Ni-SPh] in CDCl<sub>3</sub>.

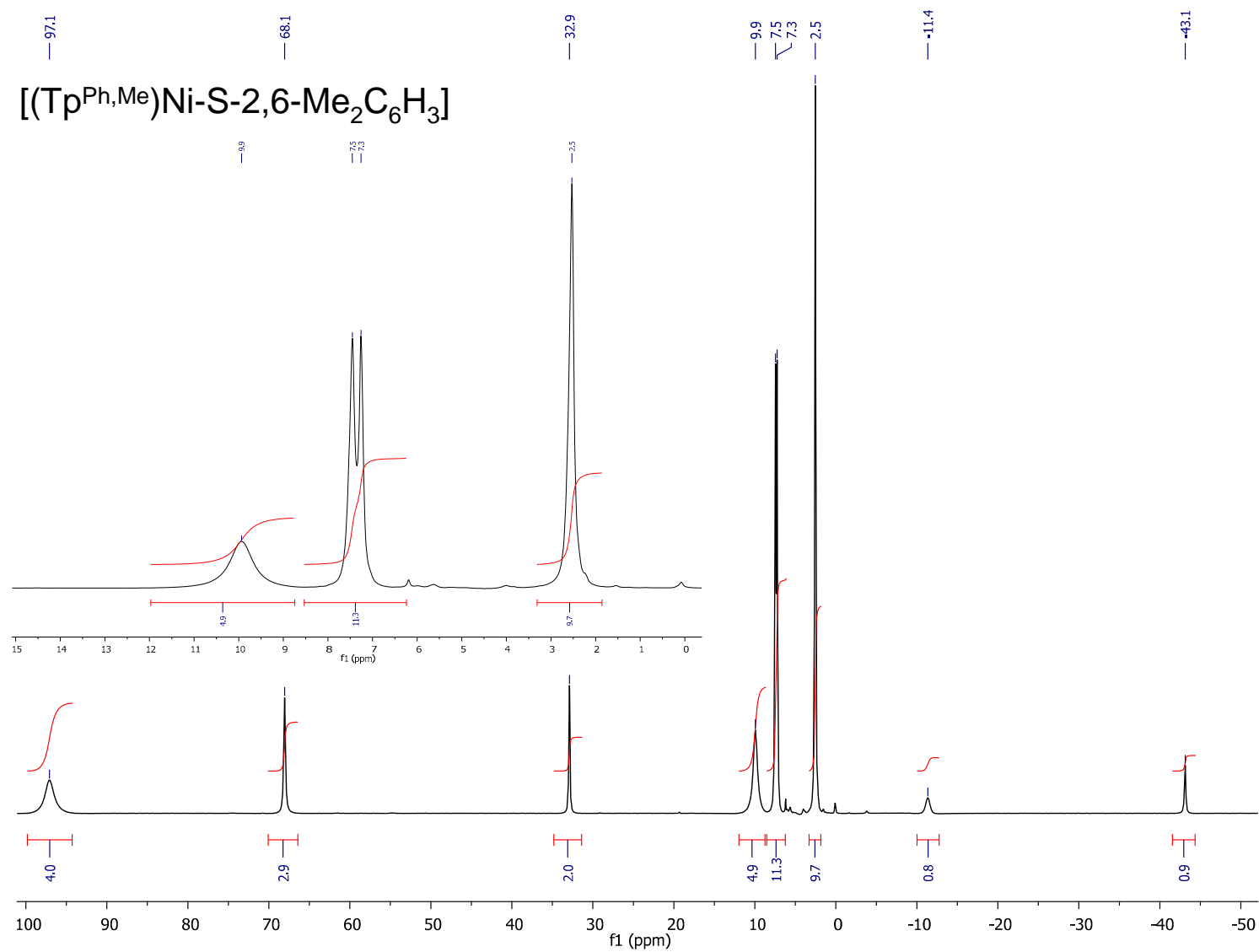


**Figure S4.**  $^1\text{H}$  NMR spectrum (500 MHz, 295 K) of  $[(\text{Tp}^{\text{Ph,Me}})\text{Ni-S-2,6-Me}_2\text{C}_6\text{H}_3]$  in  $\text{CDCl}_3$ .

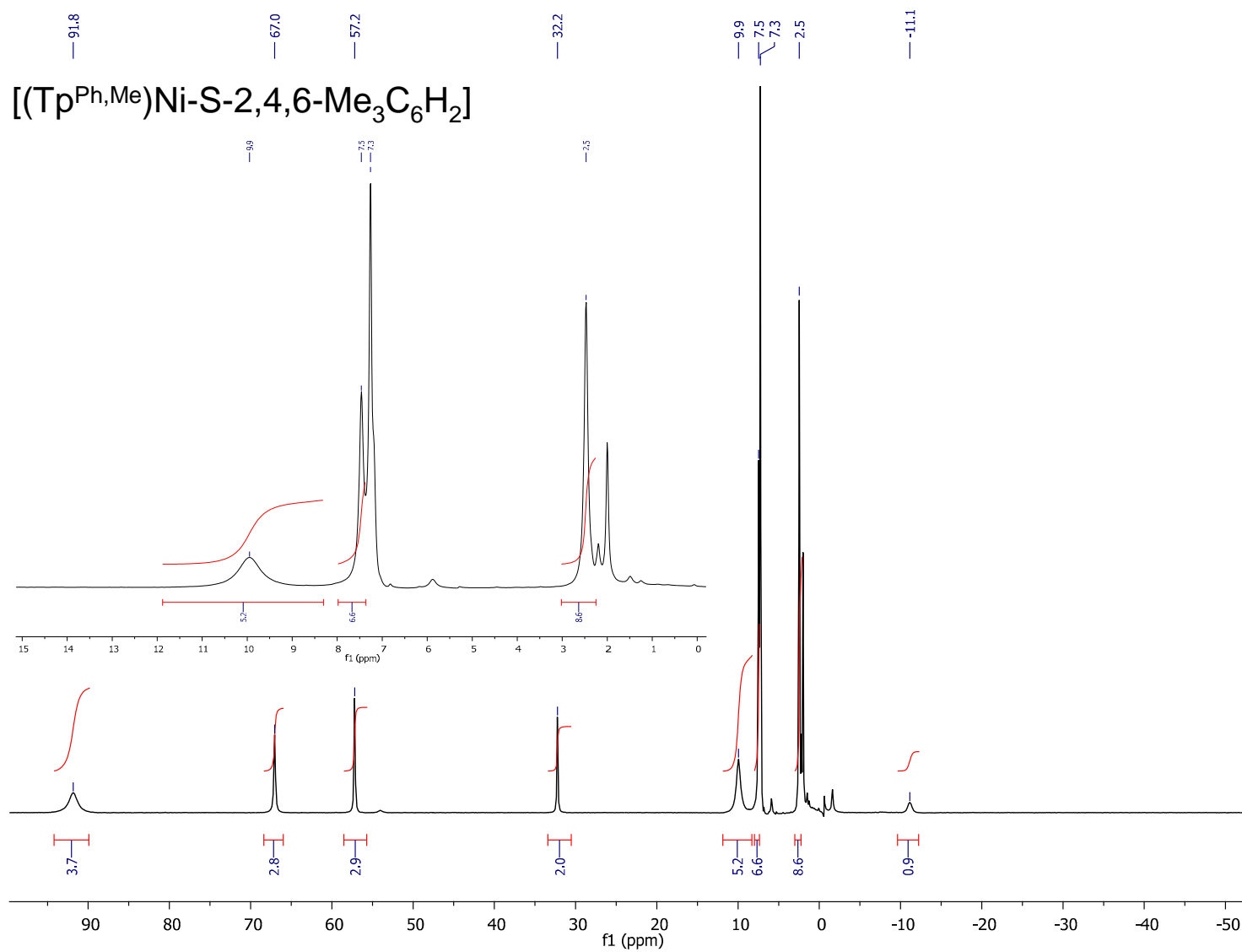


**Figure S5.**  $^1\text{H}$  NMR spectrum (500 MHz, 295 K) of  $[(\text{Tp}^{\text{Ph,Me}})\text{Ni-S-2,4,6-Me}_3\text{C}_6\text{H}_2]$  in  $\text{CDCl}_3$ .

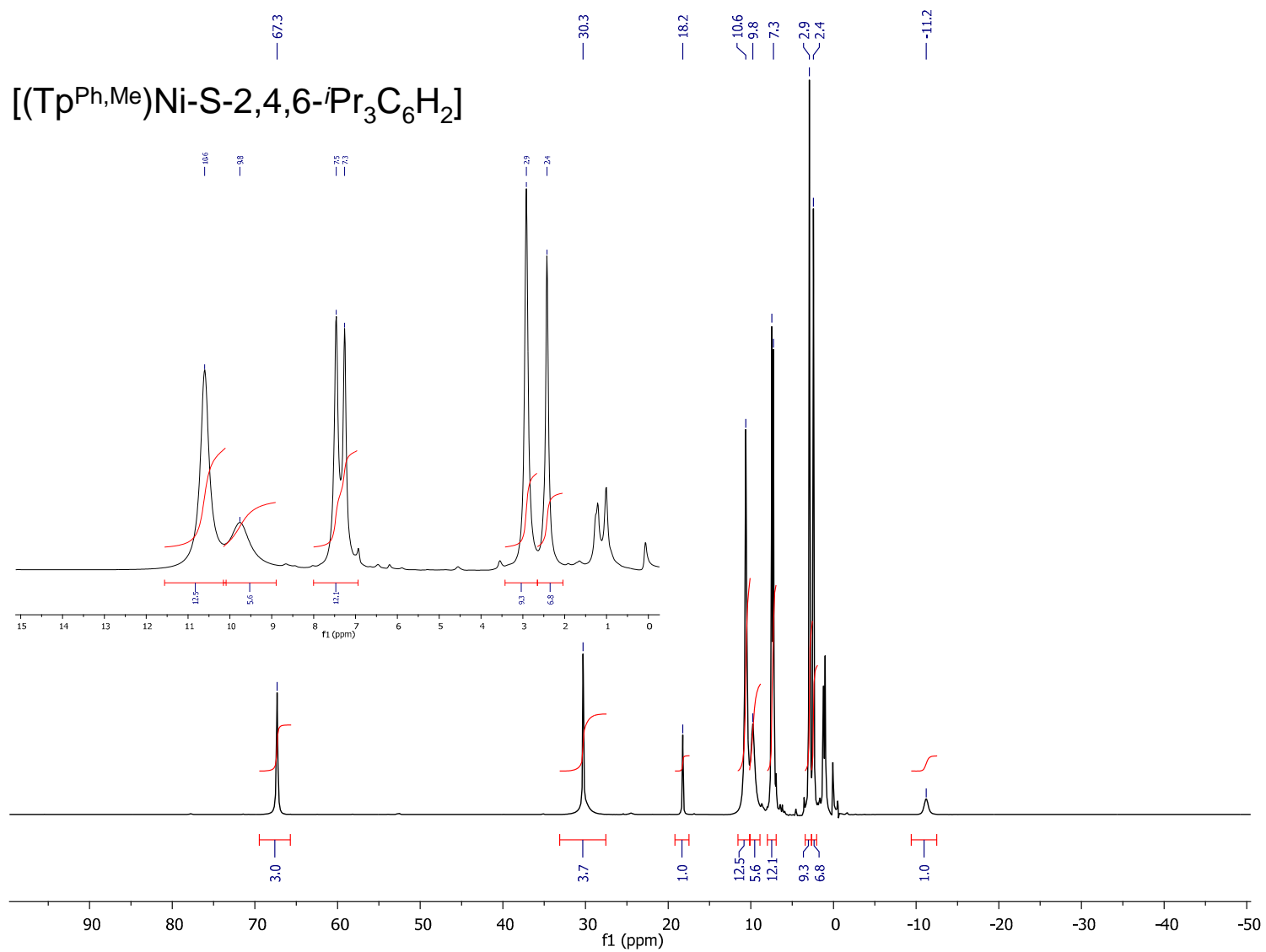


**Figure S6.**  $^1\text{H}$  NMR spectrum (500 MHz, 295 K) of  $[(\text{Tp}^{\text{Ph,Me}})\text{Ni-S-2,4,6-}i\text{Pr}_3\text{C}_6\text{H}_2]$  in  $\text{CDCl}_3$ .

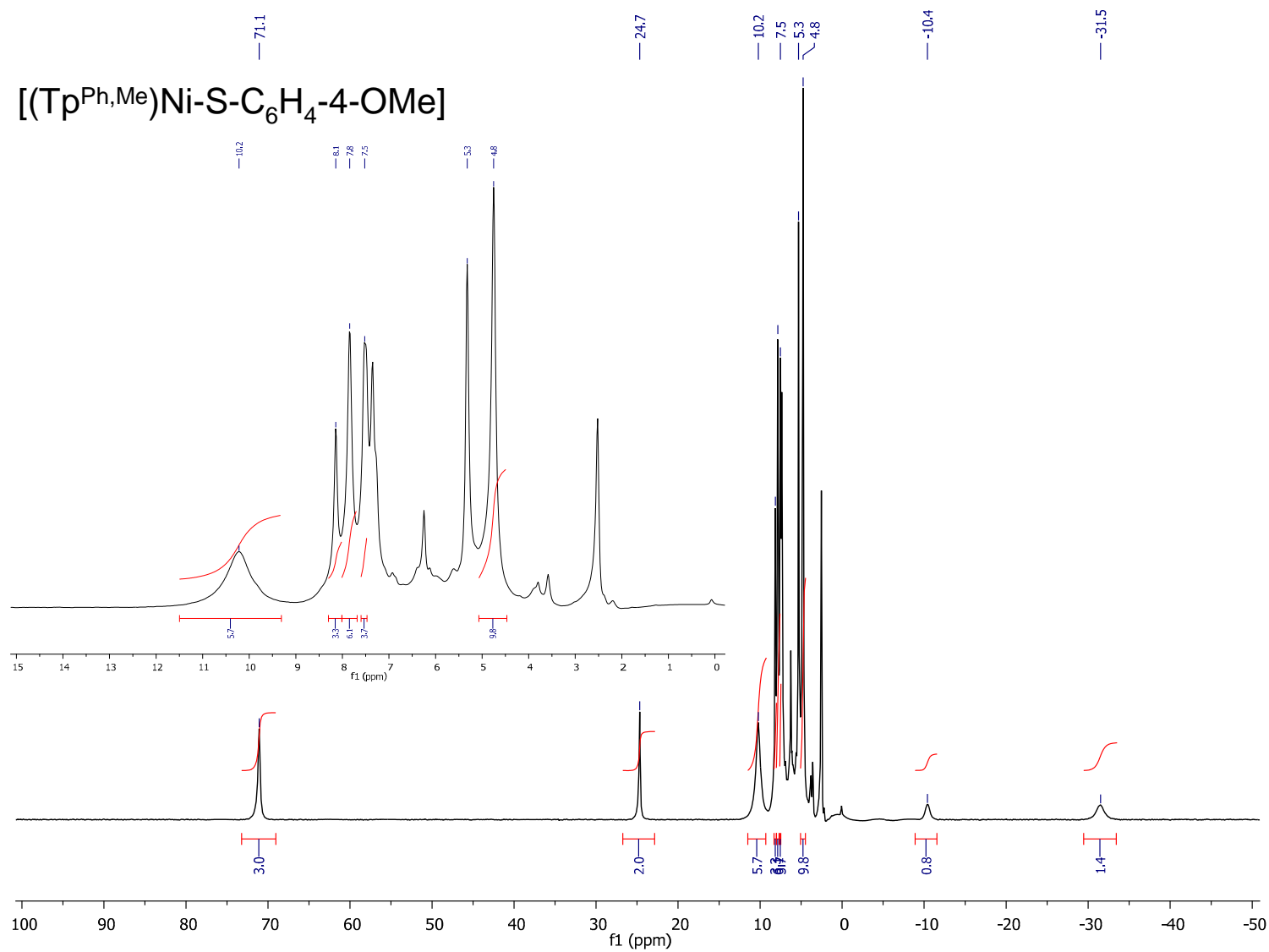


**Figure S7.**  $^1\text{H}$  NMR spectrum (500 MHz, 295 K) of  $[(\text{Tp}^{\text{Ph,Me}})\text{Ni-S-C}_6\text{H}_4\text{-4-OMe}]$  in  $\text{CD}_2\text{Cl}_2$ .

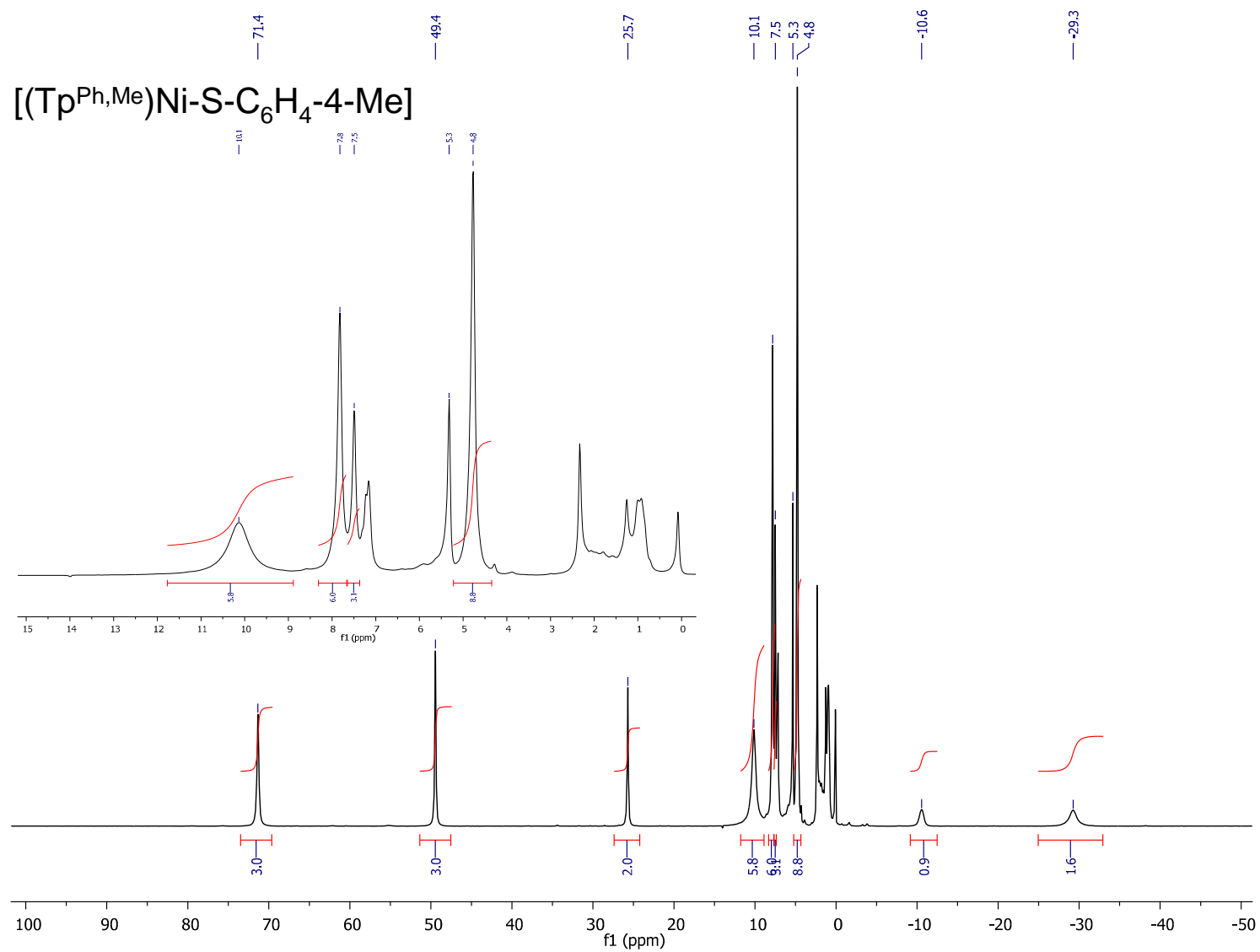


**Figure S8.**  $^1\text{H}$  NMR spectrum (500 MHz, 295 K) of  $[(\text{Tp}^{\text{Ph,Me}})\text{Ni-S-C}_6\text{H}_4\text{-4-Me}]$  in  $\text{CD}_2\text{Cl}_2$ .



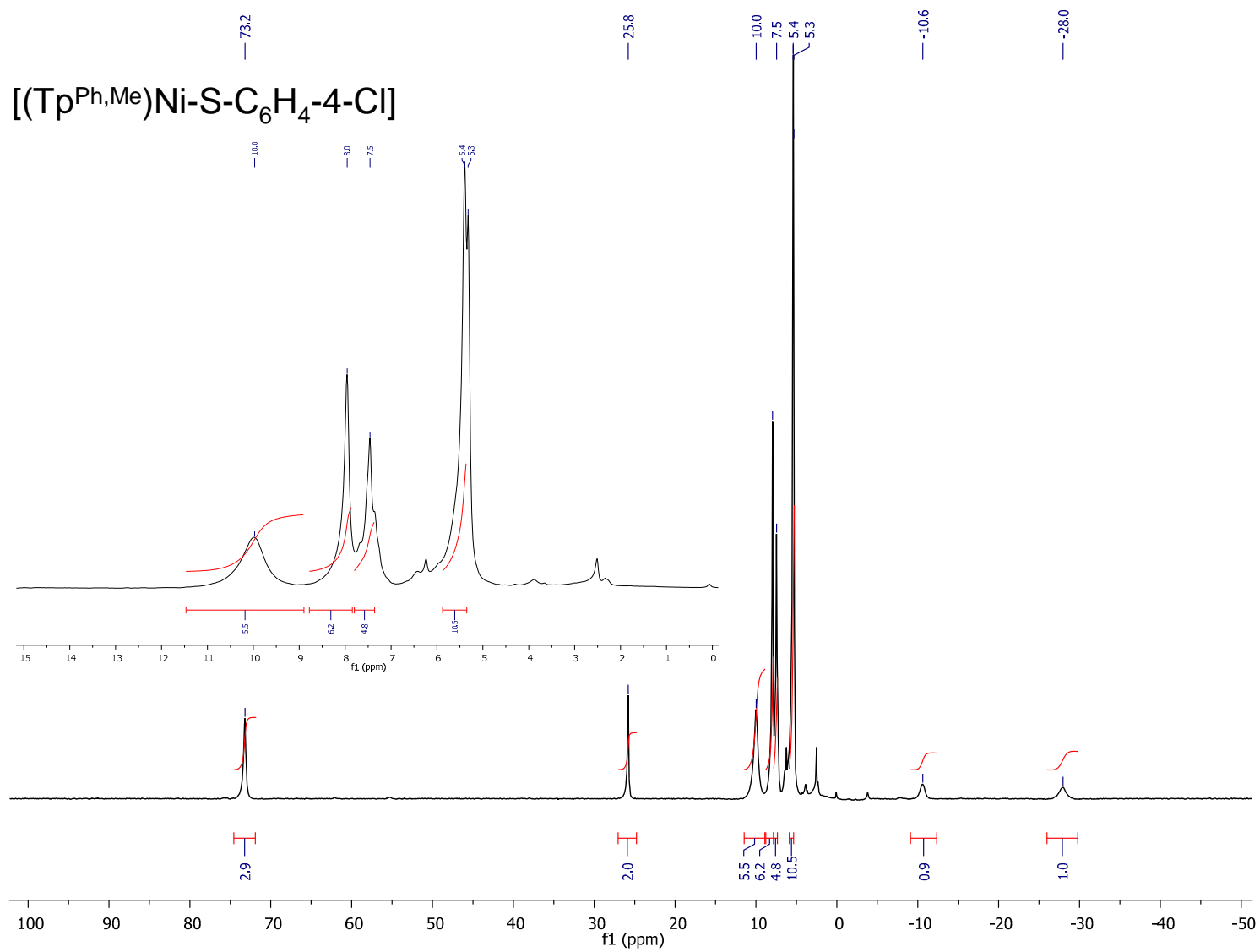


**Figure S9.**  $^1\text{H}$  NMR spectrum (500 MHz, 295 K) of  $[(\text{Tp}^{\text{Ph,Me}})\text{Ni-S-C}_6\text{H}_4\text{-4-Cl}]$  in  $\text{CD}_2\text{Cl}_2$ .

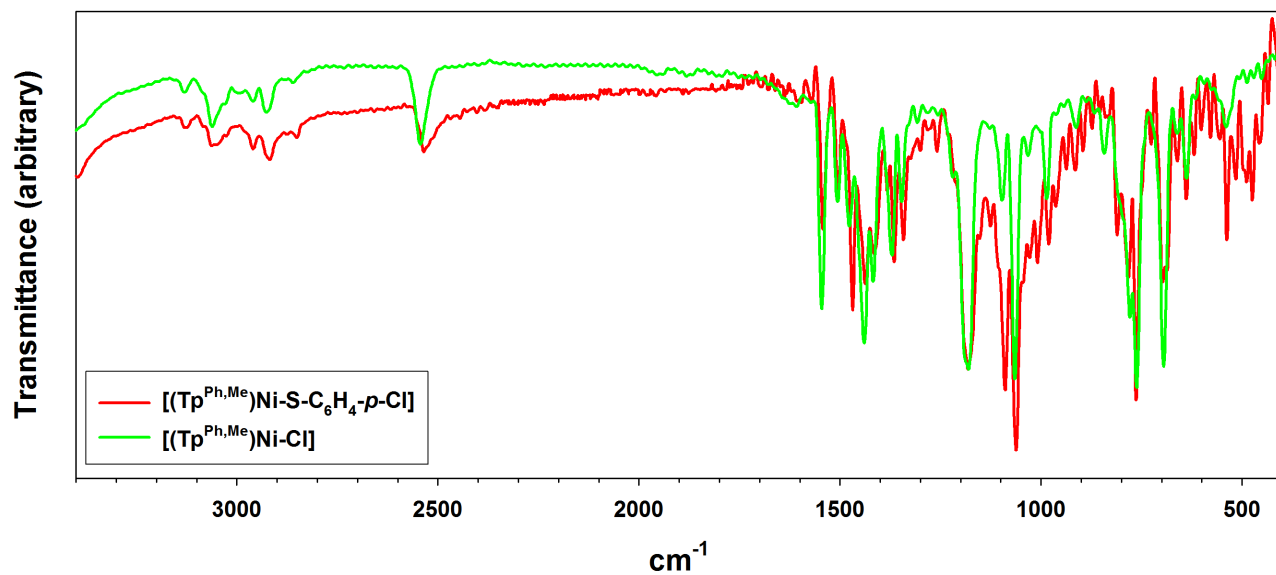


Figure S10. FTIR spectra (KBr pellets) of  $[(\text{Tp}^{\text{Ph,Me}})\text{Ni-S-C}_6\text{H}_4\text{-}4\text{-Cl}]$  (red) and  $[(\text{Tp}^{\text{Ph,Me}})\text{Ni-Cl}]$  (green).

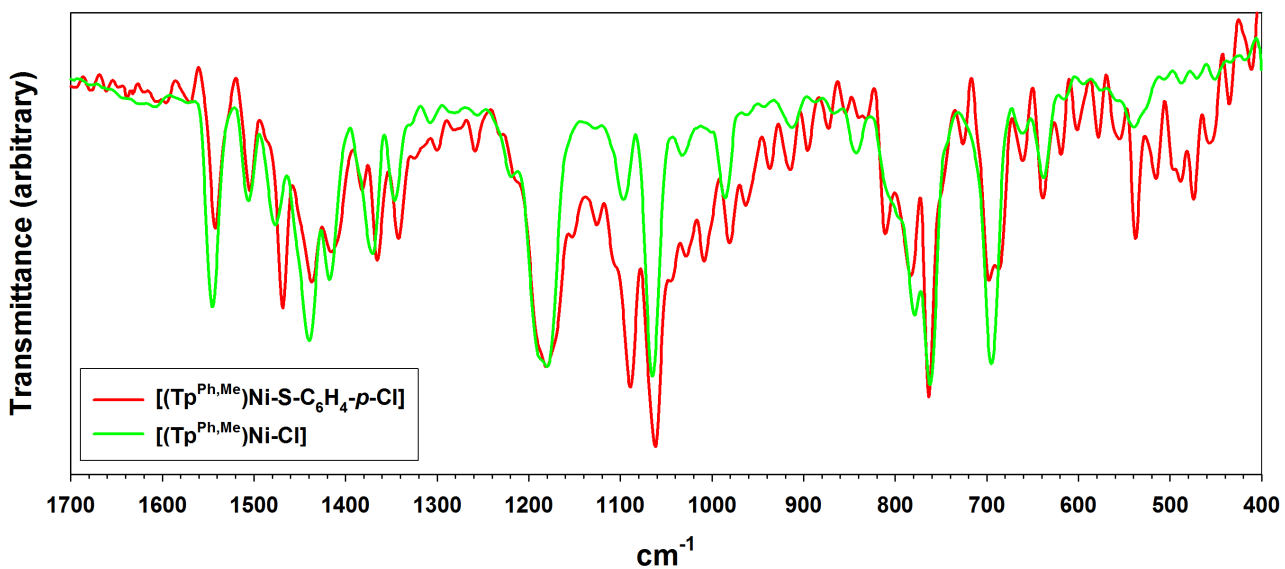
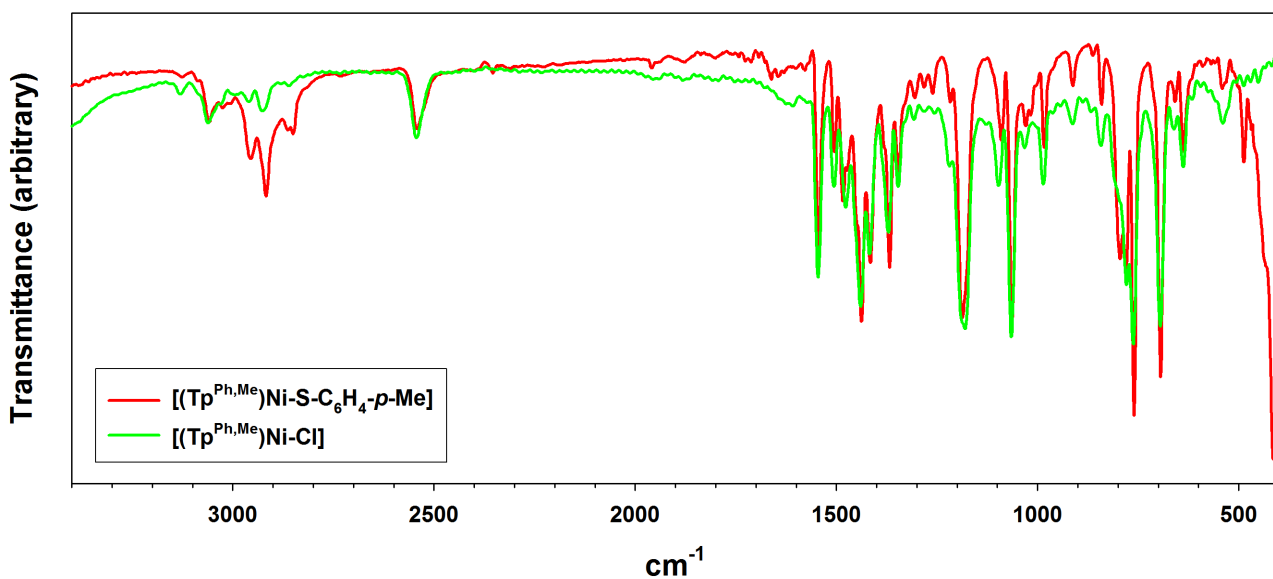
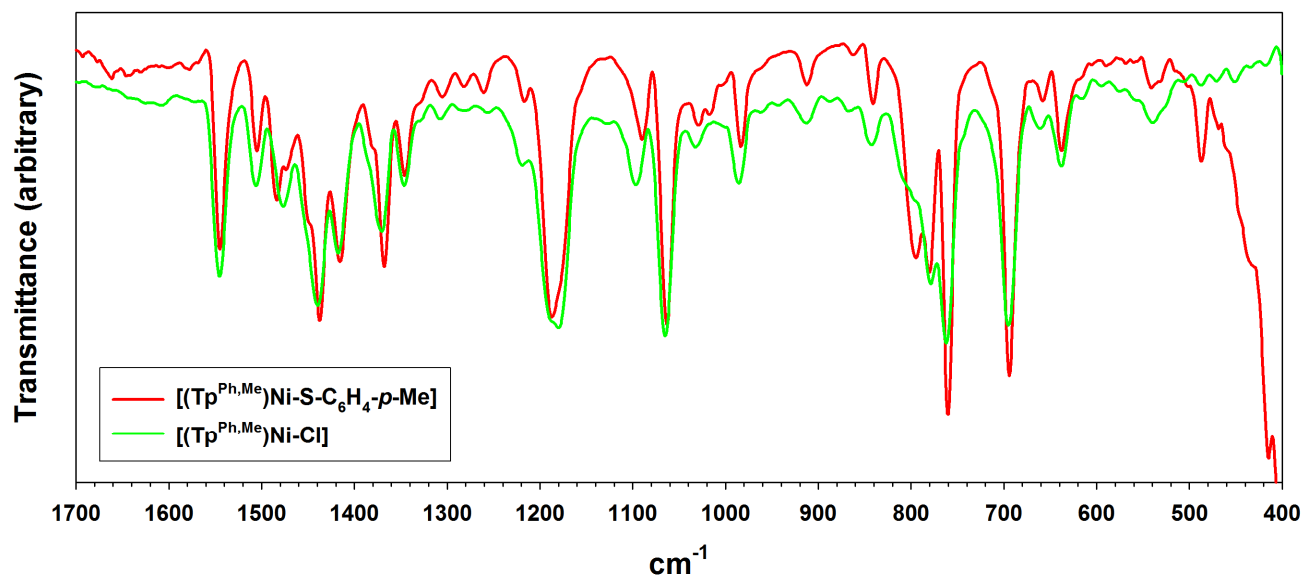


Figure S11. Detail of the FTIR spectra of  $[(\text{Tp}^{\text{Ph,Me}})\text{Ni-S-C}_6\text{H}_4\text{-}4\text{-Cl}]$  (red) and  $[(\text{Tp}^{\text{Ph,Me}})\text{Ni-Cl}]$  (green).



**Figure S12.** FTIR spectra (KBr pellets) of  $[(\text{Tp}^{\text{Ph,Me}})\text{Ni-S-C}_6\text{H}_4\text{-}4\text{-Me}]$  (red) and  $[(\text{Tp}^{\text{Ph,Me}})\text{Ni-Cl}]$  (green).



**Figure S13.** Detail of the FTIR spectra of  $[(\text{Tp}^{\text{Ph,Me}})\text{Ni-S-C}_6\text{H}_4\text{-}4\text{-Me}]$  (red) and  $[(\text{Tp}^{\text{Ph,Me}})\text{Ni-Cl}]$  (green).

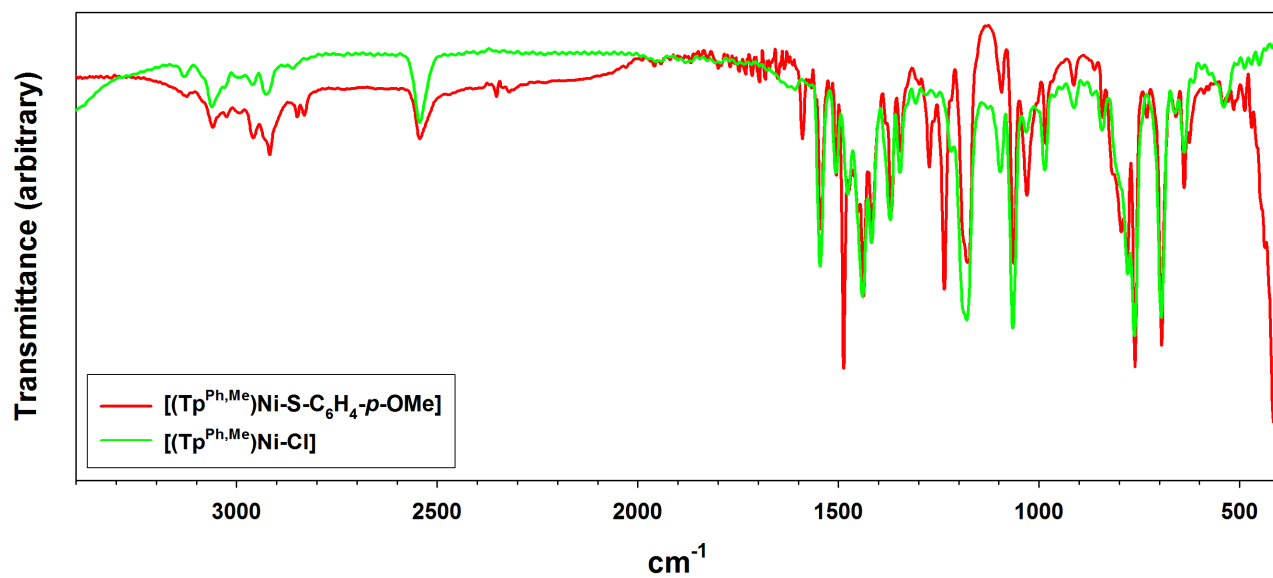


**Figure S14.** FTIR spectra (KBr pellets) of  $[(\text{Tp}^{\text{Ph,Me}})\text{Ni-S-C}_6\text{H}_4\text{-}4\text{-OMe}]$  (red) and  $[(\text{Tp}^{\text{Ph,Me}})\text{Ni-Cl}]$  (green).

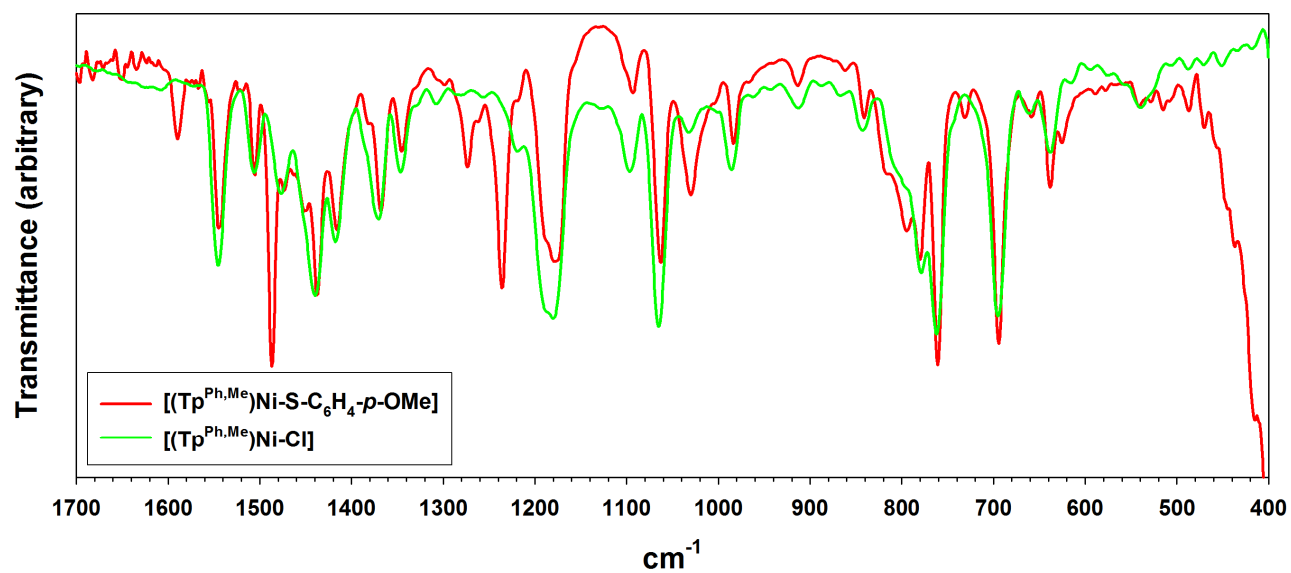


**Figure S15.** Detail of the FTIR spectra of  $[(\text{Tp}^{\text{Ph,Me}})\text{Ni-S-C}_6\text{H}_4\text{-}4\text{-OMe}]$  (red) and  $[(\text{Tp}^{\text{Ph,Me}})\text{Ni-Cl}]$  (green).

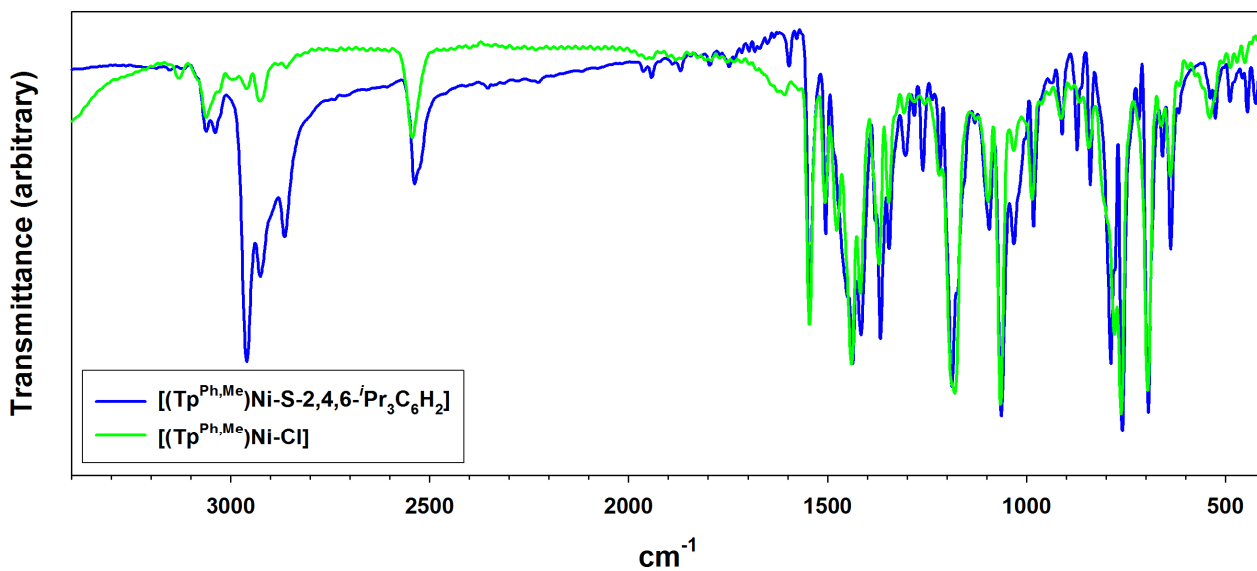


**Figure S16.** FTIR spectra (KBr pellets) of  $[(\text{Tp}^{\text{Ph,Me}})\text{Ni-S-2,4,6-}^i\text{Pr}_3\text{C}_6\text{H}_2]$  (blue) and  $[(\text{Tp}^{\text{Ph,Me}})\text{Ni-Cl}]$  (green).

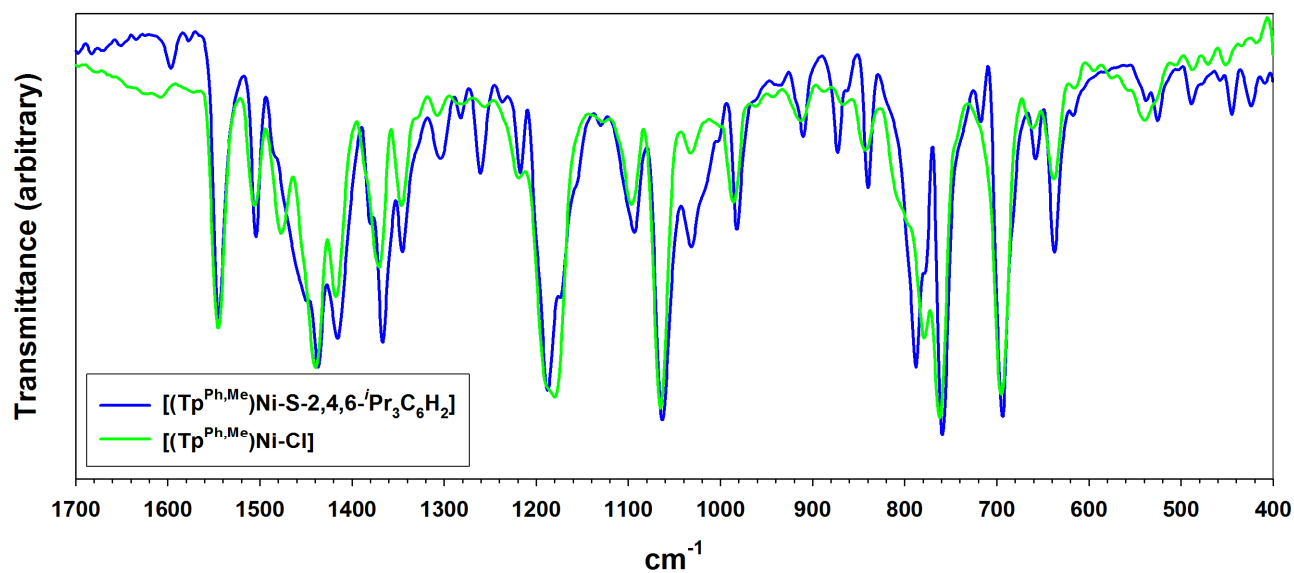


**Figure S17.** Detail of the FTIR spectra of  $[(\text{Tp}^{\text{Ph,Me}})\text{Ni-S-2,4,6-}^i\text{Pr}_3\text{C}_6\text{H}_2]$  (blue) and  $[(\text{Tp}^{\text{Ph,Me}})\text{Ni-Cl}]$  (green).

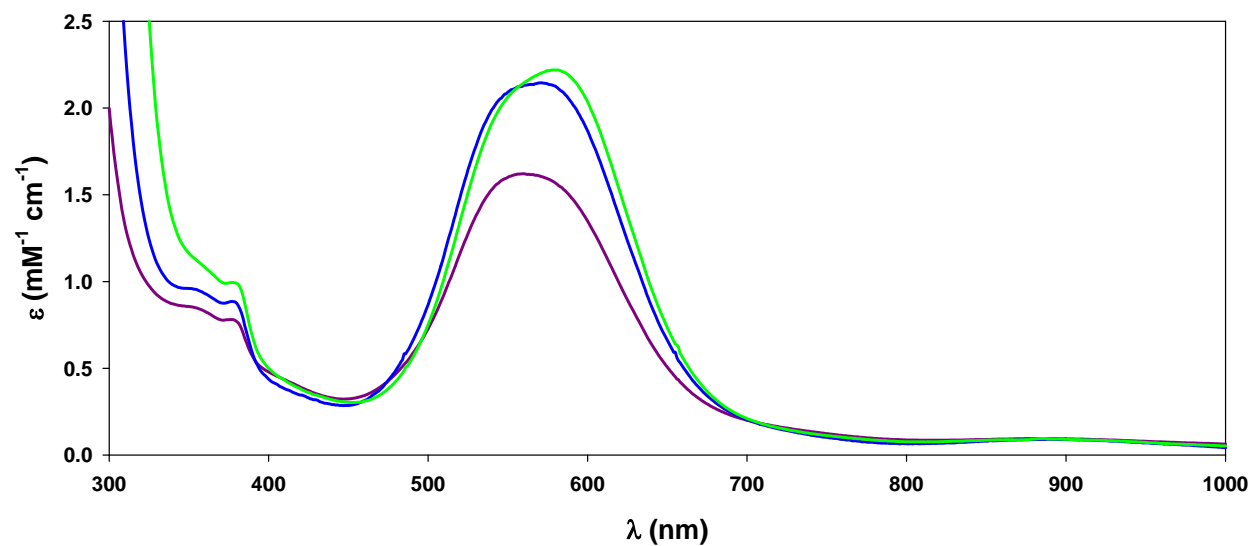


**Figure S18.** UV-Vis-NIR spectra of  $[(\text{Tp}^{\text{Ph,Me}})\text{Ni-S-2,4,6-Me}_3\text{C}_6\text{H}_2]$  at room temperature (295 K) in toluene (green),  $\text{CH}_2\text{Cl}_2$  (blue) and  $\text{CH}_3\text{CN}$  (violet) solutions.

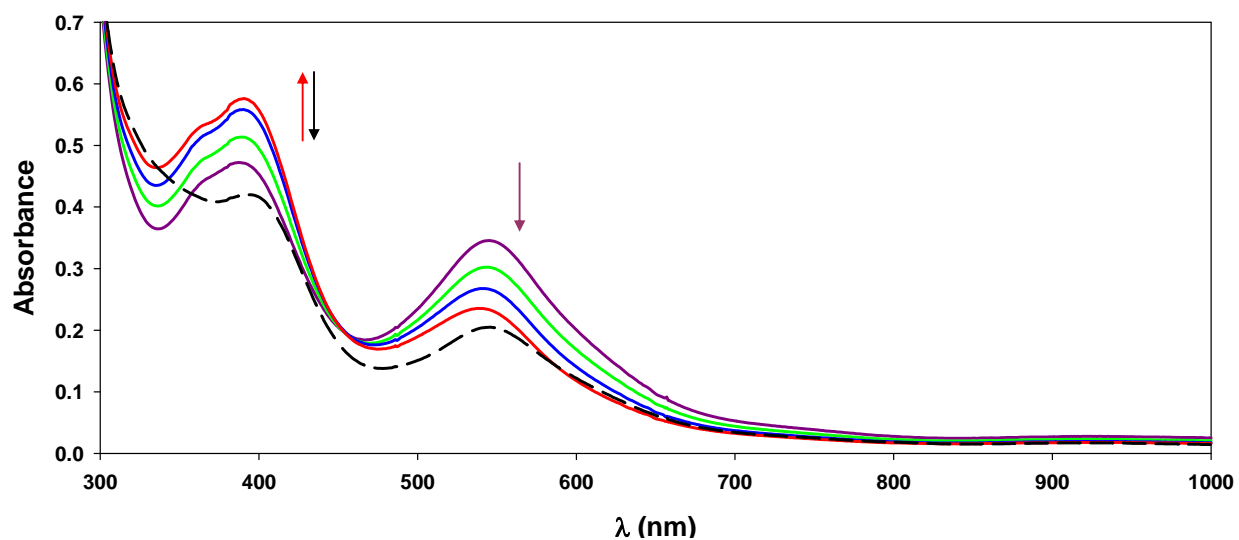


**Figure S19.** Variable temperature UV-Vis-NIR spectra of  $[(\text{Tp}^{\text{Ph,Me}})\text{Ni-S-2,4,6-}^i\text{Pr}_3\text{C}_6\text{H}_2]$  obtained with increased cooling from room temperature in  $\text{CH}_3\text{CN}$ : purple, 298 K; green, 294 K; blue, 286 K; red 278 K. The dashed black spectrum was recorded on subsequent warming to 316 K. Raw data are shown, not corrected for changes in solvent density.

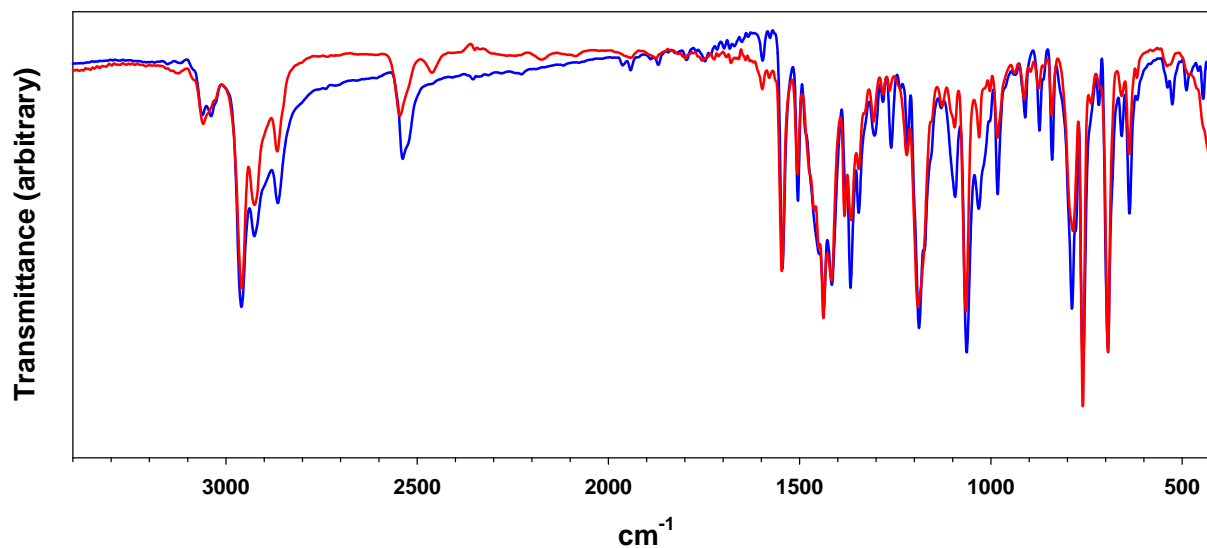


**Figure S20.** FTIR spectra (KBr pellets) of  $[(\kappa^3\text{-Tp}^{\text{Ph,Me}})\text{Ni-S-2,4,6-}i\text{Pr}_3\text{C}_6\text{H}_2]$  recrystallized from  $\text{CH}_2\text{Cl}_2/\text{hexane}$  (blue) and a mixture of  $[(\kappa^3\text{-Tp}^{\text{Ph,Me}})\text{Ni-S-2,4,6-}i\text{Pr}_3\text{C}_6\text{H}_2]$  and  $[(\kappa^2\text{-Tp}^{\text{Ph,Me}})\text{Ni}(\text{NCMe})(\text{S-2,4,6-}i\text{Pr}_3\text{C}_6\text{H}_2)]\cdot\text{MeCN}$  recrystallized from  $\text{CH}_3\text{CN}$  (red).

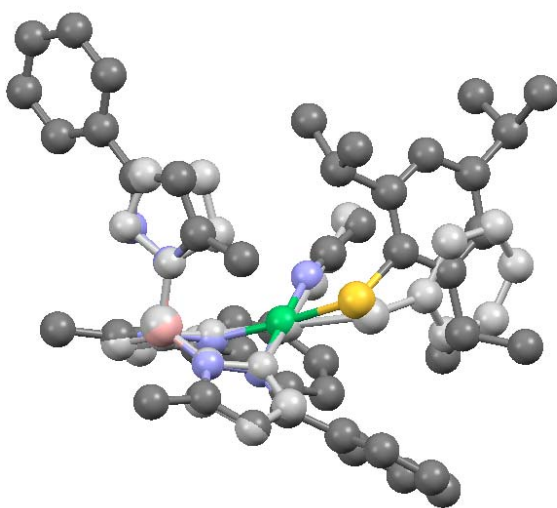


**Figure S21.** Least-squares overlay of the theoretical  $[(\kappa^2\text{-Tp})\text{Ni}(\text{NCMe})(\text{SPh})]$  model (gray) with the experimental  $[(\kappa^2\text{-Tp}^{\text{Ph,Me}})\text{Ni}(\text{NCMe})(\text{S-2,4,6-}i\text{Pr}_3\text{C}_6\text{H}_2)]$  X-ray structure (color), aligned on a common basal  $\text{BN}_3$  moiety. Hydrogen atoms are omitted for clarity.

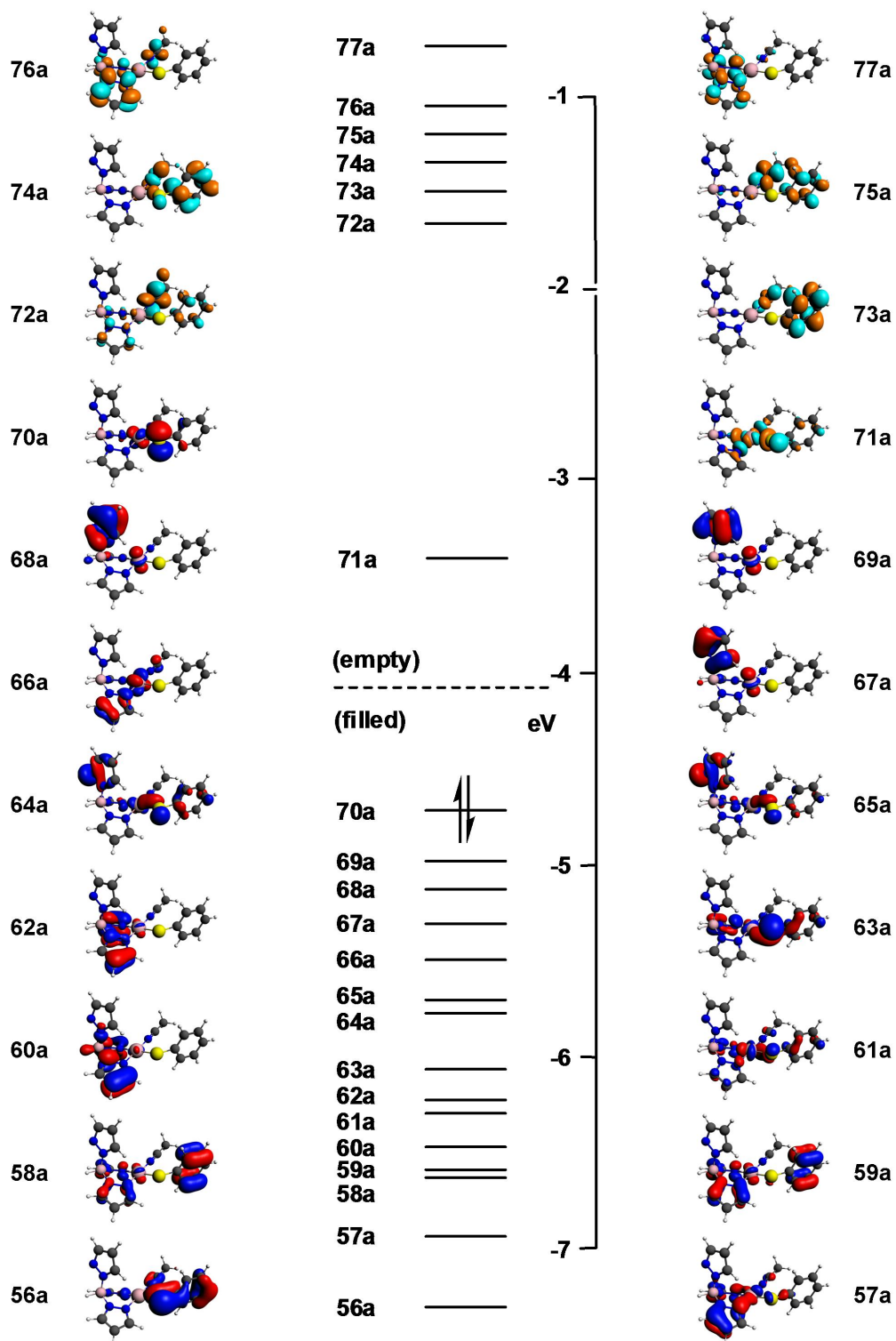


Figure S22. Frontier molecular orbitals for the  $[(k^2\text{-Tp})\text{Ni}(\text{NCMe})(\text{SPh})]$  model (see Figure S21).



**Table S1.** Coordinates for minimized structure of [(k<sup>2</sup>-Tp)Ni(NCMe)(SPh)].

	x	y	z	(Å)
Ni	0.06122635	0.04588338	0.06487979	
B	2.76893645	-1.69213365	-0.59747702	
H	3.52403892	-2.44873163	-1.14658764	
N	2.31456025	-0.62377946	-1.62548276	
N	1.21127953	0.17404010	-1.47020882	
H	3.76893866	-0.90216655	-3.13220990	
C	2.87850946	-0.36329143	-2.82805367	
C	2.13623094	0.62060750	-3.47252421	
H	2.31617368	1.05168599	-4.45090106	
C	1.09709760	0.92516206	-2.58526906	
H	0.28443444	1.63740359	-2.66979758	
N	1.49726875	-2.50453775	-0.20100405	
N	0.31948775	-1.90542667	0.12228405	
H	2.21371777	-4.49162811	-0.27847548	
C	1.36655715	-3.84523973	-0.07990942	
C	0.06511799	-4.13324240	0.32477086	
H	-0.37106661	-5.10904084	0.50889256	
C	-0.55510133	-2.88180951	0.43725324	
H	-1.57479765	-2.63504401	0.71013001	
N	3.44224546	-1.05359403	0.62430722	
N	4.17202553	-1.86764312	1.44850798	
H	2.85869438	1.01164224	0.59467469	
C	3.39284550	0.22143098	1.11293293	
C	4.11833184	0.24931573	2.29608536	
H	4.29724467	1.10857592	2.93538287	
C	4.57500207	-1.07861296	2.45415920	
H	5.18855439	-1.49640284	3.24889738	
S	-0.16676413	2.28509939	-0.05928102	
C	-1.58692984	2.84671014	0.86315136	
C	-2.90060205	2.60654640	0.41383875	
C	-3.99688094	3.12351713	1.10791706	
H	-5.00750628	2.93219474	0.74198667	
C	-3.80207119	3.90351747	2.25522698	
C	-2.50071039	4.15760893	2.70369931	
H	-2.33814960	4.77323522	3.59030093	
C	-1.40171835	3.62727810	2.02011241	
H	-3.04940414	2.01621284	-0.49163641	
H	-4.65866522	4.32006755	2.78832554	
H	-0.38615106	3.81879875	2.37016982	
N	-1.03416248	-0.02492269	1.54791722	
C	-1.66694177	-0.03268866	2.52076903	
C	-2.47240232	-0.02626339	3.72736872	
H	-3.21881832	-0.83171690	3.69286275	
H	-2.98808148	0.94102782	3.81367854	
H	-1.83086994	-0.17298850	4.60724466	

**Table S2.** Calculated excitations (TD-DFT) for [(k<sup>2</sup>-Tp)Ni(NCMe)(SPh)] model.

no.	E/eV	f/AU	Occupied to virtual orbitals	Contribution(%)
1	1.5326	0.002044	70a → 71a 69a → 71a	0.7373 0.1657
2	1.5990	0.001799	69a → 71a 68a → 71a 70a → 71a	0.4660 0.2741 0.2378
3	1.7486	0.000967	67a → 71a 68a → 71a 69a → 71a	0.4627 0.4199 0.1092
4	2.2887	0.000217	65a → 71a 64a → 71a	0.6882 0.3088
5	2.2916	0.001272	67a → 71a 69a → 71a 68a → 71a	0.4997 0.2470 0.2321
6	2.3956	0.003823	66a → 71a	0.9103
7	2.6000	0.009209	64a → 71a 63a → 71a 65a → 71a	0.4185 0.2780 0.1995
8	2.8195	0.003812	62a → 71a	0.9041
9	2.8966	0.021493	63a → 71a 61a → 71a 64a → 71a	0.3659 0.2989 0.1321
10	3.0156	0.003505	60a → 71a	0.8859
11	3.0934	0.001358	70a → 72a 61a → 71a	0.6793 0.2309
12	3.1665	0.002089	58a → 71a 59a → 71a	0.5308 0.3388
13	3.2226	0.079702	59a → 71a 70a → 73a 61a → 71a 70a → 72a	0.3153 0.2193 0.1337 0.1121
14	3.2574	0.066696	70a → 73a 61a → 71a	0.6512 0.0976
15	3.3159	0.065843	58a → 71a 59a → 71a 61a → 71a 63a → 71a	0.3048 0.2278 0.1223 0.1043

no.	E/eV	f/AU	Occupied to virtual orbitals	Contribution(%)
16	3.3275	0.011992	69a → 72a	0.8759
17	3.4247	0.002000	70a → 74a	0.8698
18	3.4642	0.000664	69a → 73a 68a → 72a	0.5509 0.4261
19	3.4716	0.002927	68a → 72a 69a → 73a	0.5135 0.4386
20	3.5074	0.018594	70a → 75a	0.8693
21	3.6030	0.009664	57a → 71a	0.9112
22	3.6136	0.000331	68a → 73a	0.9678
23	3.6254	0.000411	69a → 74a	0.9217
24	3.6519	0.000115	67a → 72a	0.9285
25	3.6599	0.004569	70a → 76a	0.9269
26	3.7189	0.000773	69a → 75a	0.9615
27	3.7683	0.001302	68a → 74a	0.9649
28	3.7905	0.000161	67a → 73a	0.9798
29	3.8612	0.000946	68a → 75a	0.9598
30	3.8764	0.000395	69a → 76a	0.9481
31	3.9258	0.016394	66a → 73a 66a → 72a	0.4733 0.4638
32	3.9456	0.000247	67a → 74a	0.9708
33	4.0111	0.030450	70a → 77a 66a → 73a 66a → 72a	0.3775 0.2924 0.1323
34	4.0279	0.000719	68a → 76a	0.8520
35	4.0384	0.008686	67a → 75a 70a → 77a	0.6159 0.1640
36	4.0428	0.014569	67a → 75a 70a → 77a	0.3491 0.2655
37	4.0727	0.000424	65a → 72a 64a → 72a	0.7958 0.1546
38	4.1105	0.001950	70a → 78a	0.9061

no.	E/eV	f/AU	Occupied to virtual orbitals	Contribution(%)
39	4.1370	0.057805	56a → 71a 66a → 74a 64a → 72a	0.4440 0.2087 0.1008
40	4.1631	0.007740	64a → 72a 66a → 74a	0.6069 0.1786
41	4.2007	0.011276	67a → 76a	0.8362
42	4.2248	0.015310	66a → 75a	0.7896
43	4.2369	0.000715	65a → 73a 64a → 73a	0.8258 0.1490
44	4.2480	0.059177	69a → 77a 66a → 74a 56a → 71a	0.2270 0.2034 0.1014
45	4.2501	0.012447	69a → 77a 66a → 75a	0.7291 0.0994
46	4.3424	0.008714	64a → 73a 63a → 72a	0.6736 0.1222
47	4.3567	0.000314	69a → 78a	0.9666
48	4.3811	0.003717	55a → 71a 65a → 74a	0.6180 0.2906
49	4.3841	0.001351	65a → 74a 55a → 71a 64a → 74a	0.4484 0.3363 0.1628
50	4.4055	0.009455	68a → 77a	0.9341